Variable switching frequency and duty cycle control strategy for the Single Active Bridge

Alexis A. Gómez, Alberto Rodríguez, Marta M. Hernando, Aitor Vázquez, Joan Giles, Javier Sebastián.

Power Supply Systems Group. University of Oviedo, Gijón, Spain.
E-Mail: gomezalexis@uniovi.es
URL: https://sea.grupos.uniovi.es/

Keywords

«Single Active Bridge», «Isolated converter», «DC-DC converter», «Switching frequency control», «DC-DC power converter».

Abstract

A new control scheme, based on variable switching frequency and duty cycle, is introduced for the Single Active Bridge converter. A static analysis is realized and a design procedure is proposed. The resulting designs are compared with previously proposed control strategies by means of simulation.

Introduction

Isolated DC – DC converters are subject to numerous developments due their relevance in popular topics such as battery chargers for electric vehicles, renewable energies or grid tied converters; the SAB converter can be considered as an interesting topology for these applications.

The Single Active Bridge converter (SAB) can be considered a variation of a Dual Active Bridge (DAB)[1]. The main difference between the DAB and the SAB is that the power flow is unidirectional due to the replacement of the secondary transistor H bridge for a full wave diode bridge or other means of passive rectification. This modification greatly simplifies the converter as there are no active switches on the secondary side, therefore no auxiliary circuitry is necessary, resulting in potentially increasing power density and reliability. Moreover, as the output bridge is passive, the control variable (phase-shift between bridges in the DAB) must be different. A general scheme of the SAB converter is shown in Fig. 1.

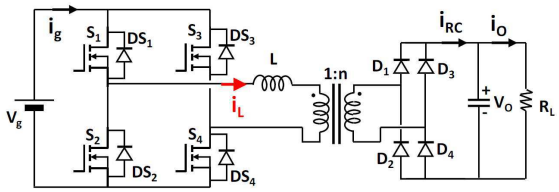

Fig. 1: Single Active Bridge (SAB) descriptive schematic.

From the static behavior, analyzed in [2]–[5], two distinct conduction modes are identified according to the inductor current (i_L) waveform. These conduction modes offer different soft-switching capabilities [6], some papers propose control and minor hardware modifications to extend the soft-switching conditions further or mitigate losses [7]–[11].

As the secondary bridge is composed by passive elements, control strategies used to extend the soft-switching conditions of the DAB, such as double or triple phase shift, are not possible. The previous literature considers the duty cycle as the only control variable of the SAB, which limits design and operation flexibility. A control scheme based on variable switching frequency and constant duty cycle was introduced in [12]. This control scheme allows operating in only one conduction mode for the entire range of operation, making possible to obtain Zero Voltage Switching (ZVS) or Zero Current Switching (ZCS) at any operating point, even at light loads.

In this document another control scheme is introduced, it uses the duty cycle and the switching frequency as control variables to provide an extra degree of freedom (DoF). This additional DoF is used to mitigate some of the drawbacks that using only one control variable had by also changing the duty cycle within a range of values that still ensures only

one conduction mode for the whole operating range.

Static analysis of the SAB and variable switching frequency

Two conduction modes, based on the inductor current waveform, are identified in the static analysis. In [6] is derived that ZVS is achievable in Continuous Conduction Mode (CCM) and ZCS is obtained when operating in Discontinuous Conduction Mode (DCM). The inductor current waveform and the soft-switching events are depicted in Fig. 2.

The SAB converter voltage conversion ratio, which is dependent on the output load for both conduction modes, corresponds to:

$$\left[\frac{V_o}{V_g}\right]_{CCM} = \frac{4n(1-d)d}{k+\sqrt{k^2+4(1-d)d}} \quad (1)$$

$$\left[\frac{V_o}{V_g}\right]_{DCM} = \frac{2nd}{d+\sqrt{d^2+k}} \quad (2)$$

being

$$k = \frac{4Ln^2}{TR_L} \quad (3)$$

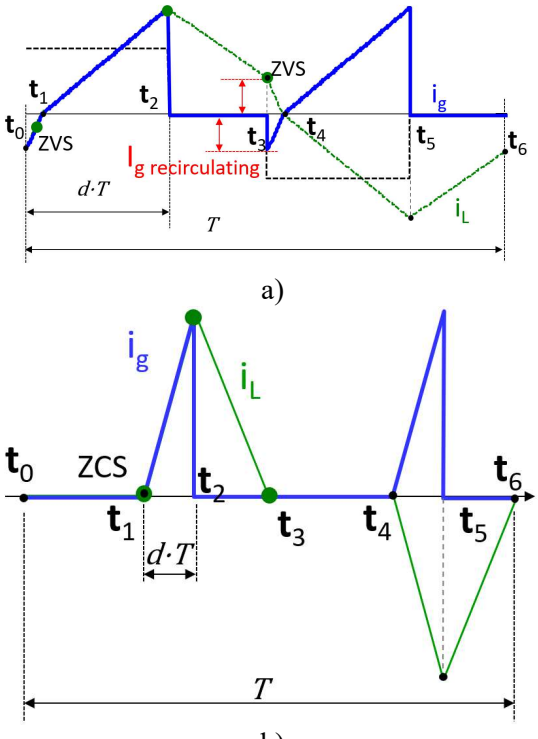

Fig. 2: Input (i_g) and inductor (i_L) currents. a) In CCM. b) In DCM

Where n is the transformer turns ratio, d is the duty cycle as defined in Fig. 2, L is the inductor value, T is the switching period and R_L is the output load.

The condition for operating in one mode or another is described by:

$$N_{crit} = \left(\frac{V_o}{V_g n}\right)_{crit} = 2\,d_{crit} \quad (4)$$

The critical duty cycle is a function of the normalized voltage conversion ratio, therefore by maintaining the duty cycle bigger or smaller than the maximum or minimum critical duty cycle, depending on the voltage range specifications and the transformer turns relation, operating only in one conduction mode is possible for the full operating range.

From equations (1) and (2) a dependency of the transferred power by the converter on the switching frequency for both conduction modes can be observed. Furthermore, the switching period only appears in (3) and shows a linear relation with the connected load. This is the basic idea behind the control strategy proposed in [12]. Maintaining a constant duty cycle that guarantees CCM or DCM operation and control the transferred power by varying only the switching frequency. Both conduction modes offer advantages and disadvantages, CCM makes possible ZVS, however there is a recirculating current that contributes to increase conduction losses; in DCM there is no recirculating current therefore, ZVS is lost but ZCS is achieved. For these reasons, the most suitable conduction mode depends on the specifications of the converter and its design goals.

For variable switching frequency and fixed duty cycle, two main drawbacks arise. The first one is that the recirculating current, necessary for ZVS, cannot be controlled. The second one is that the switching frequency range can be large.

As the duty cycle is fixed on a value, the recirculating current relative to the output current does not change with the switching frequency. So, if the recirculating current is set at minimum power to guarantee ZVS, it would result bigger than necessary at maximum

power, contributing to greater conduction losses (see Fig. 3).

The excessive switching frequency range is mainly due to the linear relation with the connected load. Therefore, there is a direct dependency of the
switching frequency range and the load variability specification.

Variable duty cycle and switching frequency strategy.

Adding a second control variable can help mitigate the previously described drawbacks associated with maintaining a fixed duty cycle.

Analyzing equations (1) and (2), the switching frequency varies inversely to the transferred power. This means that for the same duty cycle, the higher the switching frequency the less power will be transferred. On the contrary, the higher the duty cycle, the more power is transferred for a fixed switching frequency. Additionally, [12] shows that increasing the duty cycle, when operating in CCM, increases the relative recirculating current to the output current.

As in DCM there is no recirculating current, modification of either control variable only varies the transferred power and the current waveform, which can affect the efficiency of the converter. However, this is not considered in this paper and only CCM is considered, as ZVS is considered more advantageous than ZCS for the specifications of the design guide.

To minimize the switching frequency range, a duty cycle variation can be applied. At the point of minimum power, a duty cycle that guarantees CCM operation and enough recirculating current to achieve ZVS is set. To minimize the switching frequency range, the duty cycle increases for higher power levels. This makes both control variables contribute to the power transfer, resulting in a greater minimum switching frequency. As a drawback, the relative recirculating current is very sensitive to duty cycle variations when operating in CCM, therefore the average recirculating current is bigger when the duty cycle is increased for the same power level.
On the other hand, to reduce the recirculating current at high power levels, the duty cycle has to decrease as the switching frequency gets smaller. This would reduce the relative recirculating current, reducing the absolute recirculating current even though the transferred power increases. The lower limit of the duty cycle is set by the minimum necessary recirculating current for ZVS. In this occasion, both control variables are working to obtain opposite objectives. This enlarges the relative switching frequency range.

Fig. 3 shows the impact of the variation of the duty cycle on the relative switching frequency range, defined by:

$$\Delta f_{sw-rel} = \frac{f_{sw-max} - f_{sw-min}}{f_{sw-min}} \qquad (5)$$

. The relative increment of the duty cycle represents the variation of the duty cycle, positive or negative, divided by the critical duty cycle value. In Fig. 3 a), the greater the relative increment, meaning bigger values of the duty cycle at bigger power levels, the smaller the relative switching frequency range. On the contrary, in Fig. 3 b), where the duty cycle decreases from the maximum value, the greater is the decrease, the bigger is the relative switching frequency range.

For the first approach, as the recirculating current increases rapidly when the duty cycle increases, it is appropriate to maintain the minimum duty cycle value until the minimum frequency is reached. For the second approach, to maintain a small recirculating current, it is of interest to vary both control variables as the output power increases to maintain ZVS.

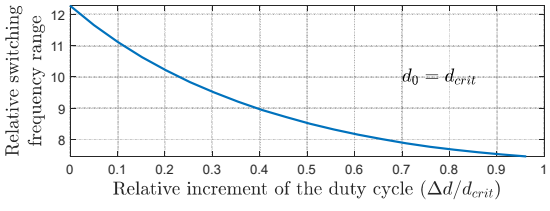

a)

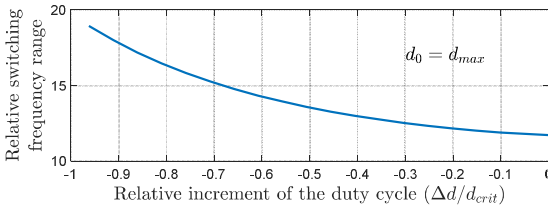

b)

Fig. 3: Relative switching frequency range as function of the relative duty cycle increment.

Ideal input and inductor current waveforms for both variable frequency control strategies with minimum recirculating current are graphed in Fig. 4.

Design guide

The design guide proposed in [12] aimed for CCM operation to achieve ZVS. Consequently, a duty cycle slightly higher than a chosen maximum critical duty cycle is selected. Once this parameter is chosen, the transformer turns relation is obtained immediately. With the condition of the minimum or maximum power point, L is determined. If the maximum and minimum switching frequencies are acceptable the design is consider valid. This design guide can be modified to implement a duty cycle increment by adding the relative switching frequency range as a final condition to the process and the duty cycle increment as a control variable.

During the design process an initial duty cycle, d_0, and a final duty cycle, d_f, will be used; the latter corresponds to d_0 plus the duty cycle maximum increment. These represent the extreme values that the duty cycle can take. This design guide is focused towards reducing the switching frequency range instead of the recirculating current, therefore d_f will be greater than d_0. The resulting design process can be summarized as follows:

1. A maximum critical duty cycle is set by the designer.

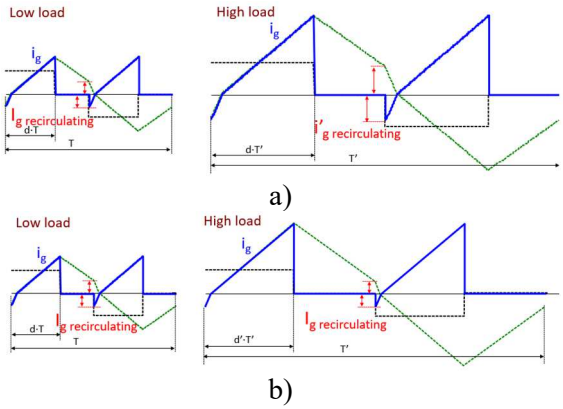

Fig. 4: Ideal input and inductor currents at different loads under different control strategies. a) Variable switching frequency and fixed duty cycle. b) Variable switching frequency and duty cycle with minimum recirculating current.

2. Considering the CCM operation requirement, equation (4) is used to determine the transformer turns relation (n).
3. The minimum duty cycle is set slightly higher than the maximum critical value to guarantee the minimum recirculating current necessary for ZVS.
4. For the minimum power operating point, the inductor value is determined using:

$$L = \left(\frac{(1-d_0)d_0}{2\,N_{min}} - \frac{N_{min}}{8}\right)\frac{\frac{V_{o\,min}}{I_{o\,min}}}{n^2 f_{max}} \qquad (6)$$

Where N_{min} is the minimum normalized voltage conversion ratio, defined as:

$$N_{min} = \frac{V_{o\,min}}{n\,V_{g\,max}} \qquad (7)$$

5. The final duty cycle value, d_f, can be determined from the maximum power point condition with the specified minimum switching frequency:

$$L = \left(\frac{(1-d_f)d_f}{2\,N_{max}} - \frac{N_{max}}{8}\right)\frac{\frac{V_{o\,max}}{I_{o\,max}}}{n^2 f_{min}} \qquad (8)$$

$$N_{max} = \frac{V_{o\,max}}{n\,V_{g\,min}} \qquad (9)$$

If the maximum duty cycle is lower than the maximum threshold, then the design is considered valid.

Although this design methodology is valid, it does not take into account the possibility of a variable duty cycle for selecting a transformer turns ratio. A bigger value of n provides smaller maximum critical duty cycles, allowing the operation with smaller duty cycles, lower recirculating currents and greater duty cycle increment. However, this increases the value of the primary side currents.

Analytical and design results

The resulting designs for the specifications of Table 1 according to different design procedures are in Table 2. The variable duty cycle is based on the design process proposed in [5], it uses the duty cycle as the only control variable and operates in both conduction modes. The variable switching frequency is

based on [12] and aims for CCM operation for any operating point, the switching frequency is considered as the only control variable. The design based on two control variables corresponds to the one proposed in this paper and explained in the previous design guide.

Table 1:Specifications for the design process

Parameter	Min	Max
Input voltages (V_g)	800 V	850 V
Output voltages (V_o)	350 V	400 V
Output current (I_o)	0.5 A	5.5 A

Table 2: Design guides results

Parameter	Variable duty cycle	Variable switching frequency	Both control variables
n	1	1	1.09
L (µH)	408	444	337
d_0	0.05	0.275	0.24
d_f	0.45	0.275	0.36
Switching frequency (kHz)	33	[22.42, 300]	[35,300]

In Fig. 5 are graphed the relative switching frequency range and the final average recirculating current of the proposed variable switching frequency and duty cycle design as functions of the initial duty cycle and the duty cycle increment. The relative switching frequency range for a given design follows:

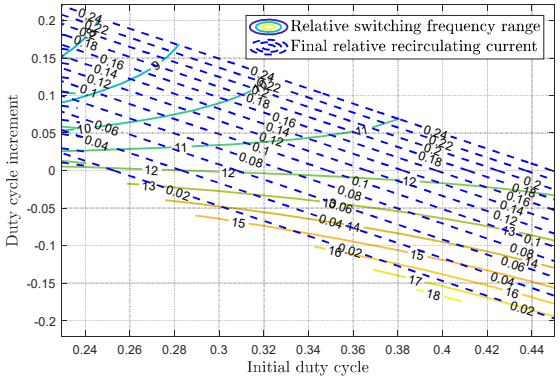

Fig. 5: Relative switching frequency range and final average recirculating current as a function of the initial and final recirculating current.

$$\Delta f_{sw-rel} = \frac{I_{o\,max} L n^2}{\sigma_1} \left(\frac{4V_{g\,max}^2 d^2 n^2 - 4V_{g\,max}^2 dn^2 + V_{o\,min}}{8 I_{o\,min} L V_{g\,max} n^3} - \frac{\sigma_1}{I_{o\,max} L n^2} \right) \quad (10)$$

$$\sigma_1 = V_{o\,max} \left(\frac{V_{o\,max}}{8 n V_{g\,min}} + \frac{V_{g\,min}\, n(d+\Delta d)(d+\Delta d-1)}{2 V_{o\,max}} \right) \quad (11)$$

and the final relative recirculating current is calculated with:

$$I_{rec\,rel} = \frac{\left(\mathrm{Vg} + \frac{\mathrm{Vo}}{n}\right)\left(d - \frac{\mathrm{Vo}}{2\,\mathrm{Vg}\,n}\right)^2}{4\,L\,f\,I_o} \quad (12)$$

The gradient color curves correspond to the relative switching frequency range defined by (5).

The dashed blue lines correspond to the final duty cycle recirculating current. This is the average recirculating current for the variable switching frequency and duty cycle design at minimum switching frequency and the duty cycle value of d_f, which in this case corresponds to the maximum power point.

From this figure two appreciations can be made, the smaller d_0, the closer the relative switching frequency range curves are, meaning that the duty cycle increment will have a greater impact for a reduced d_0 in reducing the relative switching frequency range.

On the other hand, when the duty cycle increment is positive, the relative recirculating current grows more quickly the greater the increment. These two observations confirm what was supposed for the design guide, set the duty cycle close to the maximum critical duty cycle and maintain the increment as low as possible. This means that for the design procedure, the more convenient starting point is to set a small maximum critical duty cycle value.

The proposed design is composed by simple equations with known parameters. This forces to the designer to choose certain parameters as fixed, which results in a rigid design process that many times will not achieve an optimal solution or even a solution at all. The designer must take them on an iterative process.

For the design with two control variables, as the recirculating current rapidly increases with an increase of the duty cycle while operating in CCM, control variables follow the profile depicted in Fig. 6. The duty cycle is increased when the switching frequency has reached the minimum value.

With the designs described in Table 2, a comparison of semiconductor average and RMS currents as a function of the output current is realized in Fig. 7 and Fig. 8 respectively. All currents are calculated considering the minimum specified input and maximum output voltages.

RMS and average semiconductor currents are similar for all designs. As expected from the similar results of the design processes, the two control variables design offers intermediate results in comparison with the variable only duty cycle and the variable only switching frequency designs. For the average currents, at low loads all control strategies show similar

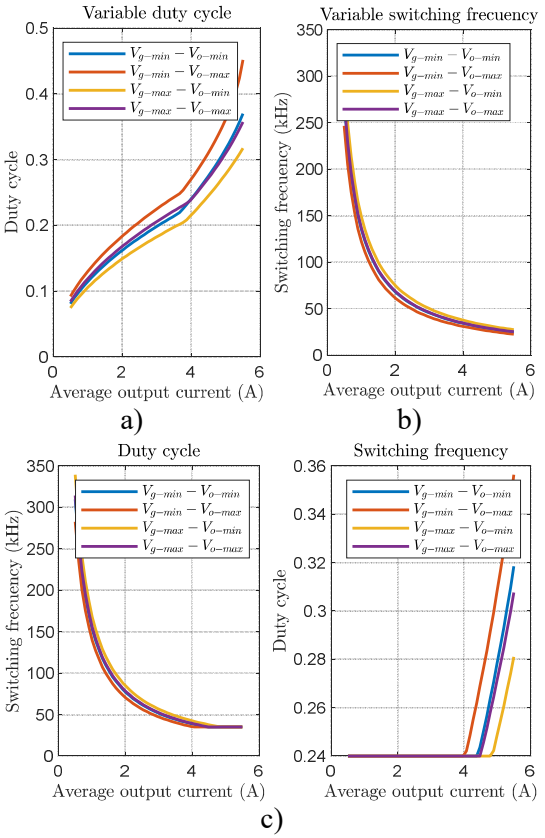

Fig. 6: Control variable curves as functions of the output current for each design. a) Variable duty cycle design. b) Variable switching frequency design. c) Variable duty cycle and variable switching frequency design (proposed in this paper)

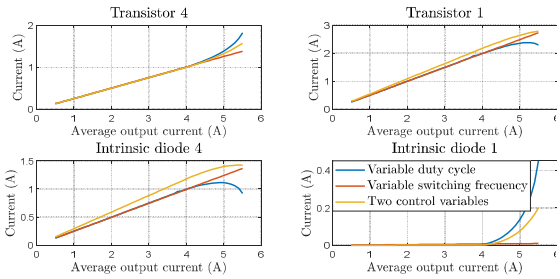

Fig. 7: Average semiconductor current comparison.

behaviors, even though they operate in different conduction modes, the designs operating in CCM do it with a small recirculating current. The one based on variable duty cycle deviates from the other two at approximately 4 A of output current. This happens because of a change in the conduction mode, from DCM to CCM; once this happens the recirculating current increases rapidly, which is visible for the intrinsic diode 1. For the RMS currents the same change in conduction mode can be observed for the intrinsic diode 1.

Additionally, for both transistors, specially at low loads for the same power, the current level is lower, this is because a more favorable current waveform results in smaller RMS currents.

Simulation results

To confirm the proposed control scheme, simulation results are used. In

Fig. 10, the control variables are plotted as function of the output current and simulation measurements of
them. In Fig. 9, two inductor current waveforms that confirm the analytical

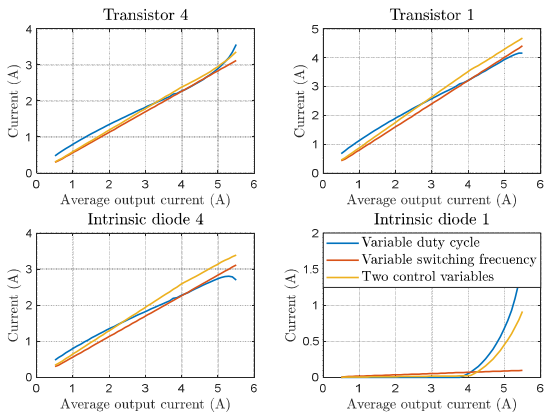

Fig. 8: RMS semiconductor current

comparison.

calculations are depicted. These results refer to the 2 variables design from Table 2. Both figures correspond to the maximum and minimum input and output voltages, respectively.

Conclusions

A new control scheme has been proposed in which the duty cycle and the switching frequency are both control variables. The additional degree of freedom can be used to reduce the switching frequency range or the recirculating current, if operating in CCM. This control strategy is confirmed and compared by means of simulation as a valid alternative that manages to expand ZVS or ZCS to the whole range of operation.

Future work includes, but is not limited to, the verification via experimental results and the extraction of an averaged small signal model of the converter controlled with variable

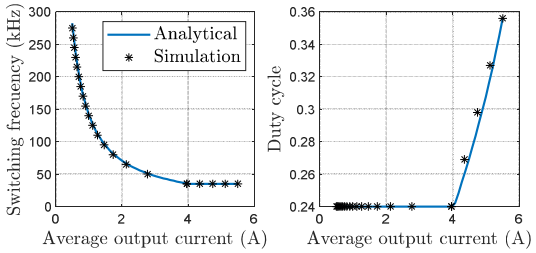

Fig. 10: Simulation validation of control variables as a function of output current.

switching frequency and with the two proposed control variables.

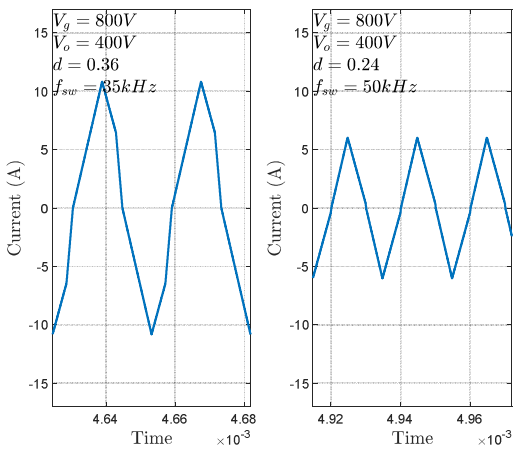

Fig. 9: Inductor current waveform for two different operating points.

Acknowledgements

This work was financed by the Spanish Ministry of Science and Innovation project MCINN-22-TED2021-130939B-I00, by the Principado de Asturias through projects SV-PA-21-AYUD/2021/51931 and PA-22-BP-21-114.

References

[1] A. Rodríguez, A. Vázquez, D. G. Lamar, M. M. Hernando, and J. Sebastián, "Different Purpose Design Strategies and Techniques to Improve the Performance of a Dual Active Bridge With Phase-Shift Control," *IEEE Trans. Power Electron.*, vol. 30, no. 2, pp. 790–804, Feb. 2015, doi: 10.1109/TPEL.2014.2309853.

[2] C. Fontana, M. Forato, M. Bertoluzzo, and G. Buja, "Design characteristics of SAB and DAB converters," in *2015 Intl Aegean Conference on Electrical Machines & Power Electronics (ACEMP), 2015 Intl Conference on Optimization of Electrical & Electronic Equipment (OPTIM) & 2015 Intl Symposium on Advanced Electromechanical Motion Systems (ELECTROMOTION)*, Sep. 2015, pp. 661–668. doi: 10.1109/OPTIM.2015.7427025.

[3] A. Averberg and A. Mertens, "Characteristics of the single active bridge converter with voltage doubler," in *2008 13th International Power Electronics and Motion Control Conference*, Sep. 2008, pp. 213–220. doi: 10.1109/EPEPEMC.2008.4635269.

[4] G. D. Demetriades, "On small-signal analysis and control of the single- and the dual-active bridge topologies," 2005, Accessed: Jan. 27, 2023. [Online]. Available: http://urn.kb.se/resolve?urn=urn:nbn:se:kth:diva-153

[5] A. Rodriguez *et al.*, "An Overall Analysis of the Static Characteristics of the Single Active Bridge Converter," *Electronics*, vol. 11, no. 4, Art. no. 4, Jan. 2022, doi: 10.3390/electronics11040601.

[6] C. Fontana, M. Forato, K. Kumar, M. T. Outeiro, M. Bertoluzzo, and G. Buja, "Soft-switching capabilities of SAB vs. DAB converters," in *IECON 2015 - 41st Annual Conference of the IEEE Industrial Electronics Society*, Nov. 2015, pp. 003485–003490. doi: 10.1109/IECON.2015.7392640.

[7] Y. Ting, S. de Haan, and J. A. Ferreira, "The partial-resonant single active bridge DC-DC converter for conduction losses reduction in the single active bridge," in *2013 IEEE ECCE Asia Downunder*, Jun. 2013, pp. 987–993. doi: 10.1109/ECCE-Asia.2013.6579227.

[8] Y. Ting, S. de Haan, and J. A. Ferreira, “Efficiency improvements in a Single Active Bridge modular DC-DC converter with snubber capacitance optimisation,” in *2014 International Power Electronics Conference (IPEC-Hiroshima 2014 - ECCE ASIA)*, May 2014, pp. 2787–2793. doi: 10.1109/IPEC.2014.6870076.

[9] C. A. Tuan and T. Takeshita, “Output Power Characteristics of Unidirectional Secondary-Resonant Single-Active-Bridge DC-DC Converter using Pulse Width Control,” *IEEJ J. Ind. Appl.*, vol. 11, no. 2, pp. 359–368, 2022, doi: 10.1541/ieejjia.21009563.

[10] S. Yamashita, K. Budo, and T. Takeshita, “Output Power Characteristics of Isolated Secondary-Resonant SAB DC-DC Converter for Output Voltage Variation,” in *2022 24th European Conference on Power Electronics and Applications (EPE’22 ECCE Europe)*, Sep. 2022, pp. 1–10.

[11] Y. Ting, S. de Haan, and J. A. Ferreira, “Elimination of switching losses in the single active bridge over a wide voltage and load range at constant frequency,” in *2013 15th European Conference on Power Electronics and Applications (EPE)*, Sep. 2013, pp. 1–10. doi: 10.1109/EPE.2013.6634627.

[12] A. A. Gómez *et al.*, “Static analysis and control strategies of the Single Active Bridge Converter,” in *2022 24th European Conference on Power Electronics and Applications (EPE’22 ECCE Europe)*, Sep. 2022, pp. 01–11.